PFC/JA-95-6

Radiative Instabilities in the Tokamak Scrape-Off Layer During Edge-Localized Mode Activity

P. Helander[1], S. I. Krasheninnikov[2],
D. Kh. Morozov*[2], T. K. Soboleva*[2]

May 1995

MIT Plasma Fusion Center
Cambridge, Massachusetts 02139 USA

*Instituto de Ciencias Nucleares,UNAM, Mexico DF, Mexico

[1]Permanent address: Chalmers University of Technology, Göteborg, Sweden
[2]Permanent address: Kurchatov Institute of Atomic Energy, Moscow, Russia

This work was supported by the US Department of Energy under contract DE-FG02-91ER-54109.

Submitted for publication in: Physics of Plasmas

Radiative Instabilities in the Tokamak Scrape-Off Layer During Edge-Localized Mode Activity

P. Helander [a], S. I. Krasheninnikov [b]

Massachusetts Institute of Technology, Plasma Fusion Center, Cambridge, MA 02139

D. Kh. Morozov [b], and T. K. Soboleva [b]

Instituto de Ciencias Nucleares, Universidad Nacional Autonoma de Mexico, Mexico D.F., Mexico

In order to reduce the heat flux entering the divertor, it is desirable to have strong impurity radiation in the scrape-off layer (SOL) of reactor-size tokamaks like the International Thermonuclear Experimental Reactor [*International Thermonuclear Experimental Reactor (ITER) Conceptual Design Activity Final Report*, ITER Documentation Series No. 16 (International Atomic Energy Agency, Vienna, 1991)]. Under such circumstances, however, the SOL plasma is likely to be unstable to the radiative condensation instability. In the present paper, an investigation is undertaken to study the effects of edge-localized mode (ELM) activity on this instability. In the linear regime, it is demonstrated that high-frequency ("grassy") ELMs may parametrically excite acoustic waves. The possibility of nonlinear radiative collapse with concomitant stratification of the plasma is discussed, and solutions describing nonlinear traveling waves are derived in which the plasma goes over from equilibrium state to another.

PACS Numbers: 52.35Mw,52.25V,52.55Fa

---

[a] Permanent address: Institute for Electromagnetic Field Theory and Plasma Physics, Chalmers University of Technology, S-412 96 Göteborg, Sweden.
[b] Permanent address: Kurchatov Institute of Atomic Energy, Moscow, Russia

I. Introduction

Enhanced confinement regimes in tokamaks are usually accompanied by Edge Localized Mode (ELM) activity.[1,2] The underlying mechanisms are still not entirely clear, but certainly involve aspects of nonlinear edge-plasma magnetohydrodynamics. ELMs introduce bursts of heat into the scrape-off layer (SOL), between which the SOL plasma cools down as a result of energy losses due to impurity radiation and heat flux to the divertor plates. Regimes where practically all the heat flux into the SOL from the bulk plasma is dissipated by impurity radiation are desirable for the divertor design for the International Thermonuclear Experimental Reactor (ITER)[3] since they are characterized by very low heat loads on the divertor plates. However, as a result of strong impurity radiation losses, the SOL plasma may be unstable to radiative instabilities. The onset of these instabilities drastically influences the nonlinear dynamics of the SOL, which is clearly important for understanding ELM phenomena and their consequences for, e.g., the ability of the divertor to cope with the incoming heat bursts.

Radiative instabilities in plasmas have been investigated by many authors in different contexts, e.g., solar prominences[4], intergalactic and interplanetary clouds,[5,6] and Multifaceted Asymmetric Radiation From the Edge plasma (MARFE) formation in tokamak plasmas[7-10] (see also references in these articles). Nearly all these studies have, however, been restricted the study of instability in systems with a stationary equilibrium. On the other hand, a tokamak SOL periodically heated by ELMs is, of course, inherently nonstationary and behaves differently. In space plasmas, one may envisage similar behavior in interstellar clouds periodically heated by pulsar radiation.

The present paper considers linear and nonlinear radiative instabilities in periodically heated, optically thin, plasmas, which are cooled by impurity radiation. There are obviously two opposite limiting behaviors of such a system. Either the plasma cools down significantly between the heat bursts, or the cooling is incomplete and the

temperature stays nearly constant. In a tokamak plasma, the first limit seems appropriate for so-called type I ELMs, where the dwell time between bursts is much longer (~30 ms in DIII-D[1]) than the duration of the bursts themselves (~1 ms). The plasma may then be unstable to the radiative condensation instability while cooling down during the dwell time. To substantiate this claim, let us make a few estimates based on parameters pertinent to the ITER. The time scales associated with convection, conduction, and impurity radiation losses are, respectively,

$$\tau_c = l_\parallel / c_s \ ,$$

$$\tau_\kappa = \frac{3 n l_\parallel^2}{\kappa}, \qquad (1)$$

$$\tau_R = \frac{3nT}{Q_R} \ ,$$

where Q_R is the energy losses owing to impurity radiation, $l_\parallel$ the characteristic length scale parallel to the magnetic field, c_s the sound speed, n the electron density, T the plasma temperature, and $\kappa \propto T^{5/2}$ the electron heat conductivity along the magnetic field lines. Numerical values for the time scales (1) with a beryllium impurity at different temperatures are presented in Fig. 1, and indicate that during the dwell time of type I ELM, after an initial phase of stable cooling down, the plasma may be unstable once the temperature becomes so low that heat conduction is small. Moreover, since τ_R is smaller than the dwell time, the instability is likely to enter a nonlinear stage. For simplicity, we have assumed that the impurity radiation can be described by coronal equilibrium, taking $Q_R = n n_I L(T)$, where n_I is the impurity density, and the function $L(T)$ depends on the impurity species.

If the repetition rate of ELM bursts is high and the amplitude is small, as in the case of "grassy" ELMs, the plasma does not have time to cool down completely or develop nonlinear instability between subsequent heat bursts. However, parametric excitation of radiative instabilities might be possible in this case.

In Sec. II we consider linear and parametric excitation of radiative instabilities. If the growth rate of the cooling-down instability from Sec. II is large compared with the inverse ELM dwell time, the instability enters a nonlinear stage considered in Sec. III. In this case, the plasma may collapse into very cold, dense regions and thus becomes highly stratified. In Sec. IV, nonlinear solutions describing nonlinear stationary thermal waves are constructed by reducing the hydrodynamic plasma equations to the Newton equation for massive particle motion in a complex potential with friction. This makes it possible to study the nonlinear stage of linear instability as well as the nonlinear instability excited by a finite amplitude perturbation. Finally, in Sec. V, our conclusions are summarized.

II. Linear radiative instability of ELMy SOL plasmas

Throughout this paper we shall describe the plasma in terms of one-dimensional hydrodynamic equations summed over all species, which for simplicity are assumed to share a common temperature and velocity. The resulting continuity, momentum and heat balance equations are

$$\frac{\partial n}{\partial t} + \frac{\partial (nv)}{\partial x} = 0 \ , \tag{2}$$

$$\frac{\partial Mnv}{\partial t} + \frac{\partial}{\partial x}\left(Mnv^2 + P - \eta \frac{\partial v}{\partial x} \right) = 0 \ , \tag{3}$$

$$\frac{\partial}{\partial t}\left(\frac{P}{\gamma-1}+\frac{Mnv^2}{2}\right)+\frac{\partial}{\partial x}\left\{\left(\frac{\gamma P}{\gamma-1}+\frac{Mnv^2}{2}\right)v-\kappa\frac{\partial T}{\partial x}-\frac{\eta}{2}\frac{\partial v^2}{\partial x}\right\}=-Q(n,P,t), \qquad (4)$$

where M and n are the averaged ion mass and density; v, P = 2nT, and T are the plasma velocity, pressure, and temperature; γ is the adiabatic index; and κ and η are the electron heat conductivity and ion viscosity coefficients. $Q(n,P,t)$ is the cooling-heating function, $Q(n,P,t) = Q_R(n,P) - Q_H(n,P,t)$, accounting for both energy losses due to impurity radiation, $Q_R(n,P)>0$, and the heat flux coming into the SOL from the bulk plasma, $Q_H(n,P,t)$, which may be strongly modulated by the ELM bursts. Since $\eta \propto P/\nu_{ii}$, we have $\kappa M \propto \eta\sqrt{M/m} >> \eta$, where ν_{ii} is the ion-ion collision frequency and m is the electron mass. When making estimates we shall assume that $Q_R = n^2\xi_I L(T)$, where $\xi_I = n_I/n$ =const. is the fraction of impurities.

If the plasma is homogeneous, $n = n_0$=const., the evolution of the pressure $P_0(t)$ is described by the equation

$$\frac{dP_0(t)}{dt} = -(\gamma-1)Q(n_0,P_0(t),t)\,. \qquad (5)$$

To examine the stability of this solution, we write $n(x,t) = n_0 + \hat{n}(t)e^{ikx}$, $P(x,t) = P_0(t) + \hat{P}(t)e^{ikx}$, where $\hat{n}$ and $\hat{P}$ are small density and pressure perturbations, and k is the wave number. Linearizing the Eqs. (2)-(4) and taking into account Eq. (5), we then obtain

$$\frac{1}{\gamma-1}\frac{d}{dt}\left\{\frac{Mn_0}{P_0(t)}\frac{d^2\hat{n}}{dt^2}+\gamma k^2\hat{n}+\frac{\eta k^2}{P_0(t)}\frac{d\hat{n}}{dt}\right\}$$

$$=-\left\{\frac{\partial}{\partial \ln P}\left(\frac{Q}{P}\right)+\frac{\kappa k^2}{2n_0}\right\}\left\{\frac{Mn_0}{P_0(t)}\frac{d^2\hat{n}}{dt^2}+\frac{\eta k^2}{P_0(t)}\frac{d\hat{n}}{dt}\right\}+\left\{\frac{\partial}{\partial \ln n}\left(\frac{Q}{P}\right)-\frac{\kappa k^2}{2n_0}\right\}k^2\hat{n}\,. \qquad (6)$$

This equation enables us to investigate radiative stability of nonstationary plasma equilibrium (5), and generalizes in this respect the earlier investigations carried out in Ref. 12. It is useful to recall the main results of these works, relevant to our further discussion, by analyzing Eq. (6) assuming that there is no time dependence of the heating-cooling function, $Q = Q_0(n,P)$. The pressure P_0=const. is then determined by the condition $Q_0(n_0,P_0) = 0$ or, equivalently, by

$$Q_R(n_0,P_0) = Q_H(n_0,P_0). \tag{7}$$

Consider the frequency $\nu_R \sim \left|\frac{\partial}{\partial \ln n}\left(\frac{Q}{P}\right)\right| \sim \left|\frac{\partial}{\partial \ln P}\left(\frac{Q}{P}\right)\right|$, which is the characteristic relaxation rate of plasma parameters due to small variations of the heating-cooling function. Since we assume that the temperatures of the different species are equal, we need to demand $\nu_R < \sqrt{m/M}\nu_{ii} \sim (m/M)\nu_{ei}$ (ν_{ei} is the electron-ion collision frequency), so that the electron-ion temperature equilibration time is smaller than the characteristic cooling time. All coefficients multiplying $\hat{n}$ in Eq. (6) are now constant, so it is worthwhile to take the Fourier transform, $\hat{n}(t) \propto e^{-i\omega t}$. Then, for high oscillation frequency, $\nu_R << \omega << \sqrt{m/M}\nu_{ii}$, the dominant terms are on the left hand side of Eq. (6), which describes adiabatic sound waves with

$$\omega = \omega_s - i\frac{(\gamma-1)^2\kappa k^2}{4\gamma n_0} - i\frac{(\gamma-1)}{2\gamma}\left\{\gamma\left(\frac{\partial Q_0}{\partial P}\right)_0 + \frac{n_0}{P_0}\left(\frac{\partial Q_0}{\partial n}\right)_0\right\}, \tag{8}$$

where $\omega_s = k\sqrt{\gamma P_0/Mn_0}$ and the subscript '0' by the derivatives indicates that they are taken at $P = P_0$ and $n = n_0$.

For small values of k, there are two additional branches in the solutionto Eq. (6), corresponding to lower frequencies, $\omega \leq \nu_R$, namely

$$\omega = \omega_P = -i(\gamma - 1)\left(\frac{\partial Q_0}{\partial P}\right)_0 , \tag{9}$$

and modified acoustic waves ($k \to 0$)

$$\omega = \omega_a + i\frac{\omega_a^2 P_0}{2(\gamma - 1)}\left\{\frac{\gamma\left(\partial Q_0/\partial \ln P\right)_0 + \left(\partial Q_0/\partial \ln n\right)_0}{\left(\partial Q_0/\partial \ln P\right)_0\left(\partial Q_0/\partial \ln n\right)_0}\right\} , \tag{10}$$

where the frequency

$$\omega_a^2 = -\frac{P_0 k^2}{M n_0}\frac{\left(\partial Q_0/\partial \ln n\right)_0}{\left(\partial Q_0/\partial \ln P\right)_0} \tag{11}$$

may be obtained from Eq. (6) by only keeping the right hand side. If $Q_R = n^2 \xi_I L(T)$, and the heating function does not depend on plasma density and pressure, Q_H const., it is useful to introduce the parameter $\beta(T) \equiv -\left(d \ln L / d \ln T\right)$. Then the relations (8)-(11) can be written in the form

$$\omega = \omega_s - i\frac{(\gamma - 1)^2 \kappa k^2}{4\gamma n_0} + i\frac{(\gamma - 1)Q_R}{2\gamma P_0}\left\{(\gamma - 1)\beta_0 - 2\right\} , \tag{12}$$

$$\omega = \omega_P = i(\gamma - 1)\frac{Q_R}{P_0}\beta_0 , \tag{13}$$

$$\omega = \omega_a + i\frac{\omega_a^2 P_0}{2(\gamma - 1)Q_R}\frac{(\gamma - 1)\beta_0 - 2}{\beta_0(2 + \beta_0)} , \tag{14}$$

$$\omega_a^2 = \frac{P_0 k^2}{M n_0}\frac{2 + \beta_0}{\beta_0} , \tag{14a}$$

where $\beta_0 = \beta(T_0)$.

From Eqs. (12)-(13) one sees that adiabatic sound wave may be unstable for $\beta_0 > 2/(\gamma - 1) > 0$, the branch ω_P is unstable for $\beta_0 > 0$, and the modified acoustic branch is unstable for $-2 < \beta_0 < 0$. The characteristic growth rate of these unstable branches is ν_R. Thus, in general a homogeneous plasma heated by a steady heat source is only stable for $\beta_0 < -2$. However, a modulation of the heat source may result in a different type of instability. Let us consider a weakly modulated heat source

$$Q_H(n, P, t) = \overline{Q}_H\left(1 + A\sin(\Omega t)\right) , \tag{15}$$

where $\overline{Q}_H$ is a constant, and A<<1 and $\Omega < \nu_R$ are the amplitude and frequency of the modulated part of the heating term. The pressure variation due to the heat source modulation follows immediately from Eq. (5)

$$P(t) \approx P_0\left\{1 + \frac{A\sin(\Omega t)}{\left(\partial \ln Q_R / \partial \ln P\right)_0}\right\} . \tag{16}$$

where P_0 is determined from relation $Q_R(n_0, P_0) = \overline{Q}_H$. Substituting expression (16) into Eq. (6) and keeping only terms linear in A, gives

$$\frac{d^2\hat{n}}{dt^2} + \omega_a{}^2\left\{1 + \hat{A}\sin(\Omega t)\right\}\hat{n} = 0, \tag{17}$$

where $\omega_a{}^2$ is defined in Eq. (11), and

$$\hat{A} = A\frac{1 + \left\{\partial\left(\ln\left(\left(\partial Q_R / \partial \ln n\right)/\left(\partial Q_R / \partial \ln P\right)\right)\right)/\partial \ln P\right\}_0}{\left(\partial Q_R / \partial \ln P\right)_0} , \tag{18}$$

or, when $Q_R = n^2 \xi_I L(T)$,

$$\hat{A} = \frac{A}{\beta_0}\left\{\frac{2(d\beta/d\ln T)_0}{\beta_0(2+\beta_0)} - 1\right\} . \qquad (19)$$

Eq. (17) describes the effect of a modulated heat source on modified acoustic waves. On the other hand, this equation is well known for its parametric instability.[13] The maximum growth rate, δ_{max}, corresponds to $2\omega_a = \Omega$ and equals

$$\delta_{max} = \omega_a |\hat{A}|/4 . \qquad (20)$$

Notice that $\delta_{max} < \omega_a \sim \Omega < \nu_R$. Taking into account the natural damping of the modified acoustic branch (See Eqs. (10), (14)), we find the following criterion for destabilization of this wave by heat source modulation

$$A > \frac{2\omega_a P_0}{(\gamma-1)Q_R}\left|\frac{\beta_0((\gamma-1)\beta_0 - 2)}{\beta_0(2+\beta_0) - 2(d\beta/d\ln T)_0}\right| \sim \frac{\omega_a}{\nu_R} . \qquad (21)$$

This inequality can be satisfied for a small modulation amplitude A because $\omega_a/\nu_R < 1$.

Since we are considering parametric excitation of a traveling wave, let us estimate the length l_a at which the parametric instability reaches its nonlinear stage. Assuming that $l_a \sim (\partial\omega_a/\partial k)/\delta_{max}$ and $2\omega_a = \Omega$, we find from Eqs. (14), (20)

$$l_a \sim c_s/\Omega A . \qquad (22)$$

For $c_s \sim 3\ 10^6$ cm^{-3}, $\Omega \sim 10^4$ s^{-1}, and $A \sim 0.1$, from Eq. (2.20) we have $l_a \sim 3\ 10^3$ cm. This estimate shows that parametric excitation of modified acoustic waves may be

important for large ITER-like devices, where the connection length of magnetic field lines in the SOL is about 10^4 cm, and the parametric instability may indeed reach a nonlinear stage.

Adiabatic sound wave can also be affected by the heat source modulation, but since $\omega_s > \nu_R$, the maximum growth rate of parametric instability is rather weak in this case, $\delta_{max} \sim A\nu_R$. In general, it can therefore not compete with the natural damping of the adiabatic sound wave $\sim \nu_R$ (see Eqs. (8)-(12)).

III. Nonlinear radiative condensation instability during the dwell time

In this Section we consider nonlinear evolution of the cooling SOL plasma during the dwell time between bursts of type I ELMs. The heat flux entering the SOL, Q_H, is assumed to be negligible between the bursts. In order to obtain a qualitative understanding of the evolution of the SOL plasma parameters, let us first, for simplicity, assume that the radiation function $L(T)$ has a power-law dependence on T over the temperature interval of interest, $L(T) \propto T^{-\beta}$. This gives the following model for the radiation function

$$Q_R(n,P) = \overline{Q}_R (n/n_0)^{2+\beta} (P(0)/P)^{\beta}, \qquad (23)$$

where $\overline{Q}_R$ is a normalization factor, and $P(0)$ is initial plasma pressure. Of course, the actual function $L(T)$ appropriate for SOL impurities cannot be described by the simple expression (23). However, analysis of plasma behavior governed by Eqs. (2)-(4) with the simplified cooling function (23) is useful for understanding more realistic cases; an example is considered at the end of this section. As we shall see, Eqs. (2)-(4) with the simplified cooling function (23) have nonlinear solutions describing the "collapse" of a plasma, unstable to the radiative condensation instability, into cold, dense filaments. Other

such solutions have been derived in various parameter regimes by Meerson and Sasorov (for cooling functions $Q_R(n,P)$ different from ours).[14-16] The first paper by these authors[14] treats the case when the cooling time τ_R is much shorter than that of heat conduction or pressure equilibration. In Sasorov's paper[15] it shown that homogeneous, cold, cylindrical regions collapse to form dense, two-dimensional surfaces, under the assumption that this process can be regarded as subsonic. This approximation is admissible for intermediate wavelengths (long enough to neglect heat conduction, but short enough to allow for pressure equilibration), as discussed in subsequent papers.[16] In contrast to these previous works, we consider non-stationary plasmas and study the nonlinear regime of the instability of a *cooling* plasma. We demonstrate that, in one dimension, thermal collapse occurs practically regardless of initial conditions if the radiation function is described by (23). Two basically different mechanisms of collapse are identified, corresponding to different ranges of the parameter β.

To proceed with the analysis, we first note that the solution of Eq. (5) describing homogeneous cooling of the plasma with the cooling function (23) is

$$P_0(t)/P(0) = \left(1 - t/t_0\right)^{1/(1+\beta)} \tag{24}$$

where t_0 is the characteristic cooling time

$$t_0 = \frac{P(0)}{\bar{Q}_R(1+\beta)(\gamma-1)}. \tag{25}$$

Note that if $\beta > -1$, the plasma cools down completely in the time t_0, whereas if $\beta < -1$, t_0 becomes negative and $P_0(t) \to 0$ only as $t \to \infty$.

As is frequently the case when analyzing one-dimensional nonlinear fluid equations, it is convenient to introduce Lagrangian coordinates (τ, z)

$$\tau \equiv t \ , \quad z(t,x) \equiv \int_0^x n(t,x')\,dx' \ . \tag{26}$$

The equations (2)-(4), where we neglect thermal conductivity and viscosity terms, then simplify to

$$\frac{\partial n^{-1}}{\partial \tau} = \frac{\partial v}{\partial z} \ , \tag{27}$$

$$M\frac{\partial v}{\partial \tau} = -\frac{\partial P}{\partial z} \ , \tag{28}$$

$$\frac{\partial \ln P}{\partial \tau} - \gamma \frac{\partial \ln n}{\partial \tau} = -(\gamma - 1)Q_R(n,P)/P \ . \tag{29}$$

At sufficiently short wavelengths, the condensation process is isobaric and subsonic, and the momentum equation (28) may be replaced by, simply,

$$\frac{\partial P}{\partial z} = 0 \tag{30}$$

When this is case (the requirements for which are discussed in detail below), the pressure is determined entirely by the conditions far from the condensation region, where we assume the plasma to be homogeneous, $n = n_\infty$=const. As a result, the pressure is given by Eq. (5) with $n=n_\infty$. If the velocity is eliminated from Eqs. (27), (29), and Eq. (5) is used for the pressure, the following equation for the density results

$$\frac{\partial N}{\partial \varsigma} = -\frac{N(N^{2+\beta} - 1)}{\gamma(1+\beta)(1+\varsigma)} \ , \tag{31}$$

where N and ς are normalized density and time variables,

$$N \equiv n / n_\infty , \qquad \varsigma \equiv -\tau / t_0(z) \tag{32}$$

Note, that if $\beta>-1$, the time variable ς runs "backwards", i.e., $\varsigma<0$ if $t>0$. The solution to Eq. (31) is

$$N(\varsigma,z) = \left[1 - \frac{1 - N_0^{-(2+\beta)}(z)}{(1+\varsigma)^{(2+\beta)/\gamma(1+\beta)}}\right]^{-1/(2+\beta)} \tag{33}$$

for arbitrary initial conditions $N_0(z) = n_0(z)/n_\infty$. It follows that, if $\beta<-2$, the homogeneous state $N=1$ is not only linearly stable, as found in the preceding secion, but also nonlinearly stable since any initial perturbation decays with time. If $\beta>-2$, and $N_0(z)>1$ for some z, the density approaches infinity there at the later instant of time

$$\varsigma = \varsigma_*(z) \equiv \left[1 - N_0^{-(2+\beta)}\right]^{\gamma(1+\beta)/(2+\beta)} - 1 . \tag{34}$$

Since the pressure is still finite, the temperature vanishes when $\varsigma=\varsigma_*$. In other words, the plasma collapses to a cold, very dense region. The collapse time $t=\varsigma_* t_0$ decreases with $N_0(z)$, so initially dense regions collapse before tenuous ones. The initial stages of a collapse with $\beta=-3/2$ is shown in Fig. 2. The density (34) is plotted as a function of x, obtained by numerically inverting the coordinate transformation (26).

To elucidate the structure of the collapsing region, suppose the initial conditions are nearly homogeneous with a small peak in the density at $z=0$, i.e.,

$$N_0(z) = 1 + \varepsilon\rho(z), \tag{35}$$

where $\varepsilon << 1$ and $\rho(z)$ has a maximum at $z=0$, where $\rho(0)=1$, and vanishes at infinity. Close to the time when the collapse at $z=0$ occurs [i.e. when $\varsigma \approx \varsigma_*(0)$], the density (33) is to the lowest order in ε equal to

$$N(\varsigma, z) = \left[\frac{1 + F(\varsigma, z)}{1 + F(\varsigma, z) - \rho(z)} \right]^{1/(2+\beta)}, \tag{36}$$

where

$$F(\varsigma, z) \equiv \left[\frac{1+\varsigma}{1+\varsigma_*(0)} \right]^{(2+\beta)/\gamma(1+\beta)} << 1. \tag{37}$$

In particular, if

$$\rho(z) \approx 1 - (z / \lambda_z)^{2g}, \quad |z| << \lambda_z, \tag{38}$$

where $g \geq 1$, the density at the time of collapse becomes

$$N(\varsigma_*(0), z) \approx (\lambda_z / z)^{2g/(2+\beta)}, \quad |z| << \lambda_z, \tag{39}$$

close to the central density peak, regardless of other initial conditions. It is now straightforward to invert the coordinate transformation (26), and express the density in terms of x:

$$N(\varsigma_*(0), x) \approx \left[\frac{2+\beta}{2(g+1)+\beta} \frac{\lambda_z}{x} \right]^{\frac{2g}{2(g+1)+\beta}}, \quad |x| << \lambda_z \ . \tag{40}$$

We are now in a position to investigate the validity of the isobaric approximation (30). If the expression for the density (36) obtained under this approximation is substituted in the continuity equation (27) and the exact momentum equation (28), the resulting velocity and pressure variation δP can be calculated. It follows that

$$v(\varsigma, z) = \frac{1}{\gamma(1+\beta)n_\infty t_0(1+\varsigma_*(0))}\int_z^\infty \frac{\rho(z')dz'}{\left[1+F(\varsigma,z')-\rho(z')\right]^{(1+\beta)/(2+\beta)}},$$

$$\delta P = M\int_z^\infty \frac{\partial v}{\partial \tau}dz', \tag{41}$$

and at the time of the collapse at $z=0$, $F \to 0$, we have

$$\frac{\delta P}{P} \sim \left(\frac{v}{c_s}\right)^2 \sim \Delta^2\left(\frac{\lambda_z}{z}\right)^{\frac{3+2\beta}{2+\beta}2g-2}, \tag{42}$$

where $c_s \equiv (\gamma P/Mn)^{1/2}$ is the local sound speed, and

$$\Delta \equiv \frac{\lambda_{x0}}{|t_0|c_0}\varsigma_*(0)^{-(\beta+3/2)/(1+\beta)} \tag{43}$$

is a dimensionless parameter. Here $c_0 \equiv c_s(n_0, P_0)$ is the sound speed at $t=0$, and $\lambda_{x0} \equiv \lambda_z/n_0$ is the length scale of the initial perturbation. It is now clear from Eqs. (42) and (43) that the isobaric/subsonic approximation (30) is valid throughout the collapse provided Δ is small and

$$\beta < \frac{2-3g}{2g-1}. \tag{44}$$

For a parabolic density maximum, $g=1$, this means that $\beta<-1$, whereas for a flat profile, $g \to \infty$, we must require $\beta<-3/2$. In addition, there is another difference in the nature of the collapse depending on whether $\beta<-3/2$. If this relation is not satisfied, the parameter Δ is only small if the scale length of the perturbation λ_{x0} is sufficiently small. But if $\beta<-3/2$, Δ can also be made small by making ε small, since then $\varsigma_*(0)$ becomes large. In other words, in the former case only perturbations of sufficiently short wavelength satisfy the isobaric approximation, whereas in the latter case it is valid for arbitrarily long-wavelength profiles provided the amplitude is small enough. It can be shown that if the initial wavelength is so large that heat conduction is negligible at $t=0$, it remains small throughout the collapse provided only $\beta<-1$. This is true even though the collapsing region shrinks during the collapse, since the temperature falls at the same time.

We now turn our attention to the case when $\beta>-1$. First of all, it should be noted that, even though the isobaric approximation eventually breaks down, as demonstrated by Eq. (42), it is still a good approximation in the early stages of the evolution of a system with isobaric initial conditions. In particular, if the parameter Δ (see Eq. (43)) is small, the density becomes significantly peaked, $N>>1$, before significant pressure variations have had time to build up. Sooner or later, however, (and always before $N \to \infty$) the pressure starts dropping, and, as a result, a collapse of a different nature takes place. This is most clearly understood by considering the limit of very long wavelengths so that the density remains nearly constant. In this case, the pressure is immediately obtained from the entropy equation (29), giving

$$P(\tau, z) = P_0(z)\left[1-\tau/t_0(z)\right]^{1/(1+\beta)}, \qquad (45)$$

just as in Eq. (24), but where P_0 now depends weakly on z. By inserting the expression (45) into the continuity and momentum equations (27), (28), the relation

$$\frac{\partial n^{-1}}{\partial \tau} = -\frac{P_0}{M}\frac{\partial^2}{\partial z^2}\int_0^{\tau}\left[1-\tau'/t_0(z)\right]^{1/(1+\beta)}d\tau' \tag{46}$$

is obtained, and it is readily verified that the density hardly changes if $\partial t_0(z)/\partial z$ is small enough. If the function $t_0(z)$ has a minimum at t =0, the pressure (45) vanishes in a region surrounding this point when $t > t_0(0)$. The plasma flows, of course, towards this region of low pressure, and it follows from the momentum equation (28) that the velocity in the cold region (where P=0) is constant in time, $v = v(z)$. As a result, the continuity equation (27) gives

$$n^{-1}(\tau, z) = n^{-1}\left[t_0(0), z\right] + \left[\tau - t_0(0)\right] v'\left[t_0(0), z\right], \tag{47}$$

predicting wave breaking and infinite density peaking when $\tau - t_0(0) = 1/(n_0 v')$. In other words, when $\beta > -1$, thermal collapse still occurs, but by a different mechanism, namely, as a result of wave breaking following the complete cooling down of the plasma.

In the case of perturbations with shorter wavelengths (but still $\beta > -1$), the nature of the collapse appears to be similar. Now the density has time to rise while the pressure is falling, but in general the pressure still goes to zero before the density becomes infinite. This can be seen from the integral of the entropy equation (29)

$$s(\tau, z) = s_0(\tau, z)\left\{1 - \frac{1}{t_0(z)}\int_0^{\tau}\left[\frac{n(\tau', z)}{n_0(z)}\right]^{(\gamma-1)(\beta_\gamma-\beta)} d\tau'\right\}^{1/(1+\beta)}, \tag{48}$$

where $\beta_\gamma = (2-\gamma)/(\gamma-1)$, $s = P n^{-\gamma}$ is (the exponential of) the entropy. It is clear that s vanishes when either $n \to \infty$ or $P \to 0$. In order for the expression (48) to vanish, however, the second term in the brackets must equal -1 if $\beta > -1$. Obviously, only very

particular choices of the function $n(\tau',z)$ approach infinity at exactly the same value of τ as this happens. (If $\beta<-1$, the integral need only diverge to ensure this behavior.) Moreover, the continuity equation (27) shows that if n approaches infinity as

$$n \propto (1-\tau/\tau_*)^{-\alpha}, \tag{49}$$

then $\alpha \geq 1$ unless $\partial v/\partial z$ becomes infinite. However, if this expression is used for n in the entropy equation (29), the pressure becomes

$$P \propto (1-\tau/\tau_*)^{[1-\alpha(2+\beta)]/(1+\beta)} \tag{50}$$

which is finite at $\tau = \tau_*$ only if $\alpha \leq 1/(2+\beta)<1$. From these considerations we can conclude that, in general, $P \to 0$ before $n \to \infty$, also for small wavelengths. After the pressure vanishes, wave breaking again occurs, which gives rise to infinite density peaking.

Finally, another interesting consequence of Eq. (48) should be pointed out. Suppose that the initial conditions are isentropic, s=const. If $\beta > \beta_\gamma$ regions with low density (= high pressure) collapse before regions with large density, but if $\beta < \beta_\gamma$ the opposite occurs. The reason for this is that adiabatic compression of the plasma increases the rate of cooling if $\beta < \beta_\gamma$ but decreases it if $\beta > \beta_\gamma$.

To summarize the results concering the nonlinear evolution of plasma cooling down according to Eq. (23), if $-2<\beta<-1$ ($-2<\beta<-3/2$ for flat profiles) the plasma collapses into a region of infinite density while the pressure remains constant. If $\beta>-1$, the pressure first vanishes, and density peaking occurs later as a result of wave breaking. Of course, the density does become truly infinite (nor does the pressure actually vanish), but is limited by processes we have ignored.

As we noted in the beginning of this Section, the impurity radiation function $L(T)$ does not in general have $L(T) \propto T^{-\beta}$, as assumed above, even though it is sometimes locally well approximated by such an expression. When the actual function $L(T)$ is used, the plasma passes through a series of stages, each of which is described by the local value of β.

Let us consider the behavior of a cooling SOL plasma in the dwell time between two (type I) ELM heat bursts ($\sim$30 ms for current tokamaks). Fig. 1, where a coronal-equilibrium model for $L(T)$ is employed, suggests that, for the parameters chosen in this figure, heat conduction stabilizes the radiation instability above $T = T_{max} = 5\,eV$. When the plasma has cooled down to this temperature, instability sets in, and any density perturbations present start growing. Since the convective (acoustic) time scale is relatively short, the process is approximately isobaric, and is described by Eq. (29) with the pressure evolution governed by the same equation taken with $n = n_\infty$. It is an easy matter to solve these equations numerically. The resulting evolution for an initially 10% density perturbation, $N=1.1$, is shown in Fig.3. Apparently, the density first peaks, but later decreases again, leaving only a comparatively small lasting trace. This behavior may be understood by considering the equation governing the density as a function of pressure,

$$\frac{\partial N}{\partial P} = \frac{N}{\gamma P}\left[1 - N^2 \frac{L(P/2n_\infty N)}{L(P/2n_\infty)}\right], \qquad (51)$$

obtained by dividing the time derivative of the density with that of the pressure. The density grows only as long as the second term in the brackets exceeds unity. But this is impossible when N becomes sufficiently large, since then $L(P/2n_\infty N)$ is quite small. The point is that $L(T)$ is *exponentially* small for low T. Therefore $\beta(T) = -d\ln L/d\ln T$ drops below the stability threshold $\beta=-2$ once the plasma becomes cold enough. After this has happened, the region of rarefied plasma surrounding the collapse cools down faster than the collapsing

region, "sucking out" plasma from the latter. As a result, the density peaking decreases. However, since the cooling is now quite slow, residual plasma stratification may persist for a long time. For instance, in the example shown in Fig. 3, $N>3$ still after 30 ms. This may strongly affect the dynamics of the next ELM burst.

IV. Nonlinear propagating thermal fronts in the SOL during ELMs

In the preceding sections we have considered the effects of heat flux modulation due to ELMs. However, ELM bursts are characterized not only by an increase of the heat flux entering the SOL plasma, but also by a sizable particle flux from the bulk into the SOL. In the present section we show that this may result in the formation of nonlinear propagating thermal waves. Related waves were studied in Refs. 6 and 17.

Let us consider subsonic plasma flow with the plasma parameters only depending on the single variable $\xi = x - Vt$, where V=const.>0. In a frame moving with the velocity V, assuming that the pressure is almost constant, $P \approx P_0$=const., and uniform plasma parameters at $|\xi| \to \infty$, we find from Eqs. (2)-(4)

$$\frac{d}{d\xi}\left(\kappa\frac{dT}{d\xi}\right) - \frac{\gamma j_\infty}{\gamma - 1}\frac{dT}{d\xi} = \hat{Q}(T) , \qquad (52)$$

where $\hat{Q}(T) \equiv Q\left((P_0/2T), P_0\right)$ and j_∞=const. is the plasma flux at $\xi \to \infty$. Generally speaking, the function $\hat{Q}\left(T_{eq}\right) = 0$ may have a complicated dependence on the plasma temperature, and have several equilibrium states,

$$\hat{Q}\left(T_{eq}\right) = 0 , \qquad (53)$$

characterized by different temperatures T_{eq}. As we shall see, Eq. (52) describes a nonlinear propagating thermal front separating one equilibrium state characterized by the temperature $T_{eq,1}$, to another one with the temperature $T_{eq,2}$.

Introducing the function $\vartheta(\xi)$ by $d\vartheta = \kappa(T)dT$, we can write Eq. (52) in the more convenient form

$$\frac{d^2\vartheta}{d\xi^2} = -\frac{\partial U(\vartheta)}{\partial\vartheta} - \mu(\vartheta)\frac{d\vartheta}{d\xi} , \tag{54}$$

which is similar to the equation of frictional motion of a particle (ϑ is the "coordinate" of the particle and ξ is the "time") in the effective potential

$$U(\vartheta) = -\int_{T_{eq}}^{T(\vartheta)} \hat{Q}(T')\kappa(T')dT' , \tag{55}$$

where the "friction" coefficient $\mu(\vartheta) \propto j_\infty$ is determined by the expression

$$\mu(\vartheta) = -\gamma j_\infty / (\gamma - 1)\kappa(T(\vartheta)) . \tag{56}$$

An equation similar to Eq. (54) was derived in Ref. 17, where the authors, having in mind a specific form of the effective potential $U(\vartheta)$, concluded that the front-like solution of Eq. (54) is uniquely determined by the function $U(\vartheta)$. As we shall see, this appears not to be true in general.

Let analyze the solution of Eq. (54) with the function $U(\vartheta)$ shown in Fig. 4 where the local maxima of $U(\vartheta)$ correspond to $\vartheta_1 = \vartheta(T_{eq,1})$ and $\vartheta_2 = \vartheta(T_{eq,2})$. At high temperatures $U(\vartheta) \to \infty$ since we expect the cooling function to vanish, leaving $Q = -Q_H < 0$.

We seek a solution switching the plasma from ϑ_1 to ϑ_2, so the energy loss due to "friction" has to make up for the "potential energy" difference between these states

$$\Delta U = U(\vartheta_2) - U(\vartheta_1) \tag{57}$$

(in our particular case $\Delta U<0$). However, if the "friction force" is weak, a "particle" starting the motion from the "coordinate" ϑ_1 may pass through the "coordinate" ϑ_2 and be reflected by the "potential" $U(\vartheta)$ near the "coordinate" ϑ_3 where $U(\vartheta_3) \approx U(\vartheta_1)$ (see Fig. 4). Thus, the "particle" might make many bounces between points ϑ_1 and $\bar{\vartheta}_1$ until it arrives at the point ϑ_2 (with zero "velocity", $d\vartheta/d\xi=0$). In this case one can use perturbation theory to determine the flux j_∞ as a function of the number of oscillations J_b in the potential well (in the limit $J_b>>1$). From Eq. (54) we find the variation of the "energy", $\Delta E = (d\vartheta/d\xi)^2 / 2$, for one bounce (back and forth) between the points ϑ_1 and ϑ_3

$$\Delta E = \frac{2\gamma j_\infty}{\gamma - 1} \int_{\vartheta_1}^{\vartheta_3} \left\{ \sqrt{2|U(\vartheta)|} / \kappa(\vartheta) \right\} d\vartheta \ . \tag{58}$$

If the "potential energy" difference ΔU is small in comparison with the depths of the potential wells in the range $\vartheta_1 < \vartheta < \vartheta_3$, we can use the estimate (58) for all the oscillations the particle executes until arriving at ϑ_2. Then, from Eqs. (57), (58) we find

$$j_\infty = \frac{(\gamma - 1)\Delta U}{2\gamma J_b} \left\{ \int_{\vartheta_1}^{\vartheta_3} \left\{ \sqrt{2|U(\vartheta)|} / \kappa(\vartheta) \right\} d\vartheta \right\}^{-1} \ . \tag{59}$$

Thus, we see that Eq. (52) allow a family of front-like solutions taking the plasma from one equilibrium state $T_{eq,1}$ to another one $T_{eq,2}$ through many oscillations between temperatures $T_{eq,1}$ and $T_{eq,3}>T_{eq,2}$, where $T_{eq,3}$ corresponds to ϑ_3. The question of stability of these solutions requires further investigation, and is beyond the scope of the present paper.

V. Conclusions

Let us summarize the general results of this paper and their relevance to present and future tokamak experiments. As pointed out in the introduction, a SOL plasma cooled by impurity radiation is highly likely to be unstable to the radiative condensation instability, at least in the temperature interval surrounding the peaks in the radiation functions of any impurities present. In Sec. II the linear stage of the instability is investigated. When high-frequency ("grassy") ELMs are present, parametric excitation of modified acoustic waves appears to be possible. This is probably harmless in present-day devices since the propagation length (22) required for significant amplification of the wave is quite long, but may be of importance in reactor-size experiments. On the other hand, nonlinear radiative condensation can probably occur in the dwell time between the bursts of type I ELMs, even in relatively small tokamaks. For cooling functions of the form $L(T)\sim T^{-\beta}$, where $\beta>-2$, this inevitably leads to a localized thermal collapse of the plasma into very dense, cold filaments (by different mechanisms depending on whether $\beta>-1$). More realistic cooling functions (e.g., corresponding to coronal equilibrium) are peaked around one or several temperatures, below which they approach zero very quickly. This leads to more complicated behavior of the condensing region, with the plasma typically first contracting and then expanding again. It is then a matter of time scales what the consequences are. If the plasma is still stratified when the next ELM burst strikes, its dynamics can be expected to be significantly affected.

For instance, since the radiation function is proportional to n^2, an inhomogeneous plasma radiates more than a homogeneous one with the same average density. It should be noted that to observe the filamentation in numerical simulations might require a very fine mesh since the condensation length scale may be quite small.

ELM bursts involve both heat and particle fluxes. In Sec. IV, nonlinear solutions describing travelling thermal waves are derived. These waves are characterized by different temperatures in front of and behind the wave, are associated with fluxes of both heat and particles, and may describe the behavior of the SOL plasma when suddenly heated by an ELM burst.

Acknowledgments

S.I.K. is pleased to acknowledge the hospitality and support of the Instituto de Ciencias Nucleares, Universidad Nacional Autonoma de Mexico at Mexico City, where this work was initiated.

This work was performed in part under Department of Energy grant DE-FG02-91-ER-54109. PH was supported by the European Community under an association contract between Euratom and Sweden, and by a fellowship from the Swedish Institute.

References

[1] D. N. Hill et al., J. Nucl. Materials **196-198**, 204 (1992).

[2] H. Zohm, F. Wagner, M. Endler, J. Gernhardt, E. Holzhauser, W. Kerner, and V. Mertens, Nucl. Fusion **32**, 489 (1992).

[3] *International Thermonuclear Experimental Reactor (ITER) Conceptual Design Activity Final Report*, ITER Documentation Series No. 16 (International Atomic Energy Agency, Vienna, 1991).

[4] E. Tandberg-Hassen, *Solar Prominences* (Reidel, Dordrecht), 1974.

[5] L. Spitzer, *Physical Processes in the Interstellar Medium* (Wiley, New York), 1978.

[6] A.G. Doroshkevich and Ya. B. Zel'dovich, Zh. Eksp. Teor. Fiz. **80**, 801 (1987) [Sov. Phys. JETP **53**, 405 (1981)].

[7] T. E. Stringer, in *Proceedings of the 12th European Conference on Controlled Fusion and Plasma Physics* (European Physical Society, Budapest), Part I, 1985, p. 86.

[8] B. Lipshultz et al., Nucl. Fusion **24**, 977 (1984).

[9] J. Neuhauser et al., Nucl. Fusion **26**, 1697 (1986).

[10] J.F. Drake, Phys. Fluids **30**, 2429 (1987); J. F. Drake, L. Sparks, and G. van Hoven Phys. Fluids **31**, 813 (1988).

[11] V. A. Abramov et al., *Proceedings of the 20th European Conference on Controlled Fusion and Plasma Physics* (European Physical Society, Lisboa), Part II, 1993, p. 823.

[12] G. B. Field, Astrophys. J. **142**, 531 (1965).

[13] L. D. Landau and E. M. Lifshitz, *Mechanics* (Pergamon Press, Oxford, 1976), p. 80.

[14] B. I. Meerson and P. V. Sasorov, Zh. Eksp. Teor. Fiz. **92**, 531 (1987) [Sov. Phys. JETP **65**, 300 (1988)].

[15] P. V. Sasorov, Pis'ma Astron. Zh. **14**, 306 (1988) [Sov. Astron. Lett. **14**, 129 (1988)].

[16] B. Meerson, Astrophys. J. **347**, 1012 (1989); I. Aranson, B. Meerson, and P. V. Sasorov, Phys. Rev. E **47**, 4337 (1993).

[17] A. M. Dimits and B. Meerson, Phys. Fluids B **3**, 1420 (1991).

Figure Captions

1. The characteristic times of convection (τ_{co}), conduction (τ_K), and energy losses (τ_r) due to radiation from 0.2% beryllium in an ITER-like SOL plasma, $n_e=10^{20}\,m^{-3}$, $l_{//}=30m$.

2. Isobaric collapse with $\beta=-3/2$, i.e. $L(T)\sim T^{3/2}$, with an initial density profile $N_0(x)=1+0.2\,[\exp(-x^2) - \exp(-x^2/4)/2]$, $\gamma=5/3$. The curves show N(t,x) for t=0, t=20 $|t_0|$, and t=60 $|t_0|$.

3. Time evolution of a density perturbation N(t), with N(0)=1.1 in a plasma cooling down from T(0)=5 eVwith 0.2% Be impurity, $n_e=10^{20}\,m^{-3}$.

4. Frictional motion of a particle in the potential $U(\vartheta)$, describing a thermal wave connecting regions with equilibrium temperatures ϑ_1 and ϑ_2.

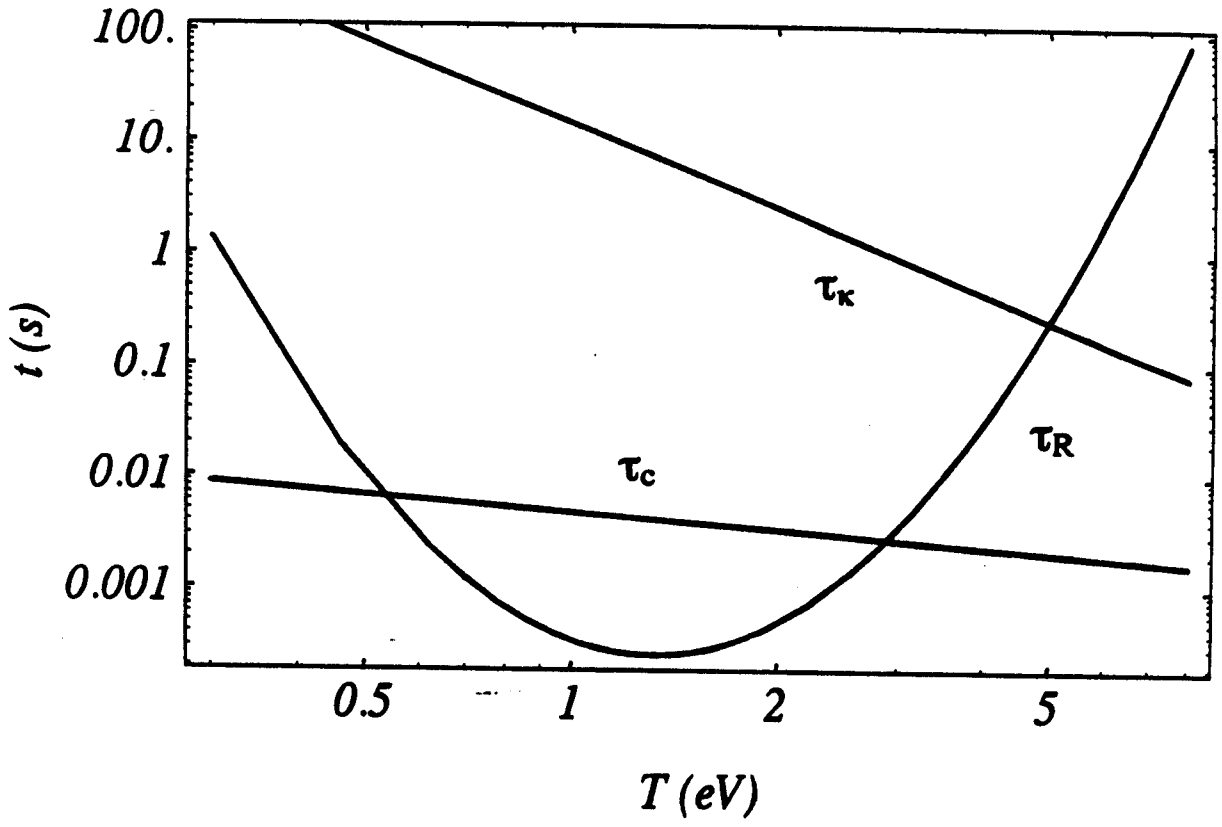

Fig. 1

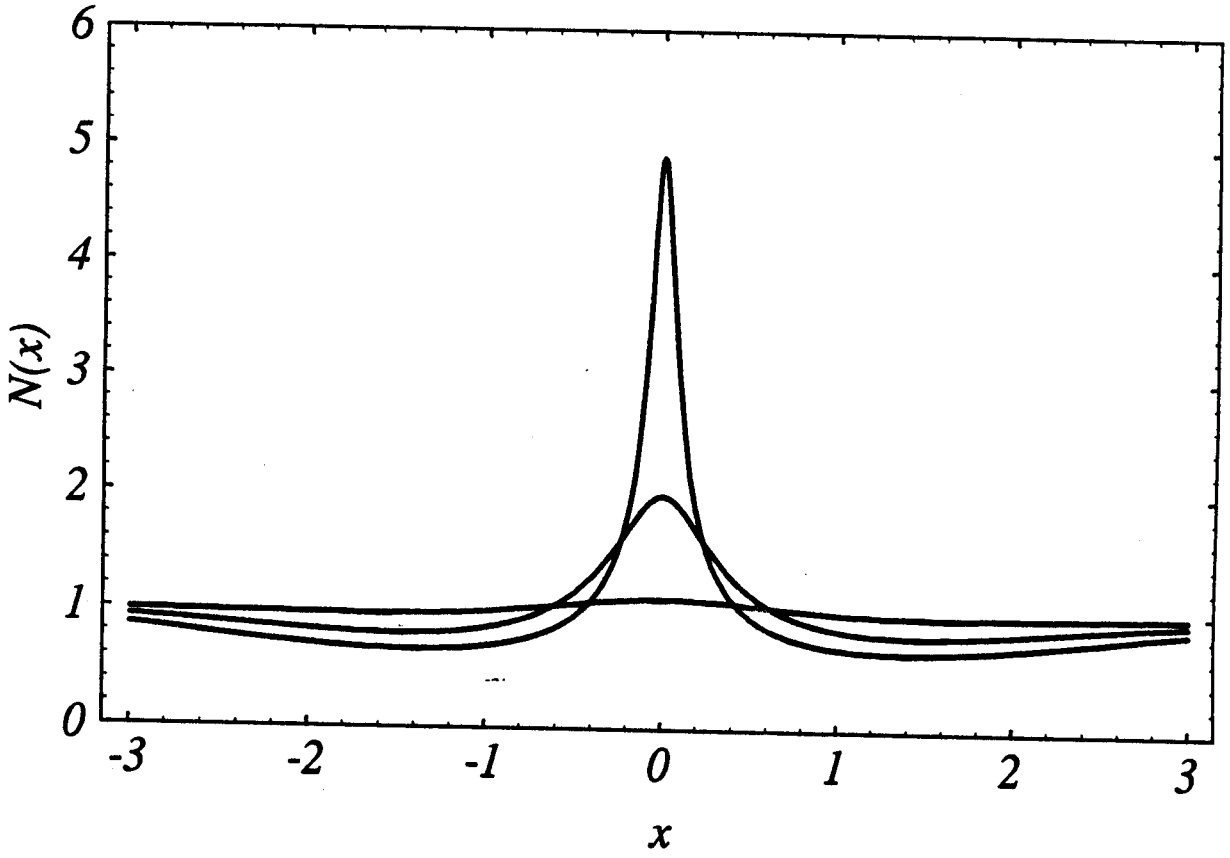

Fig 2.

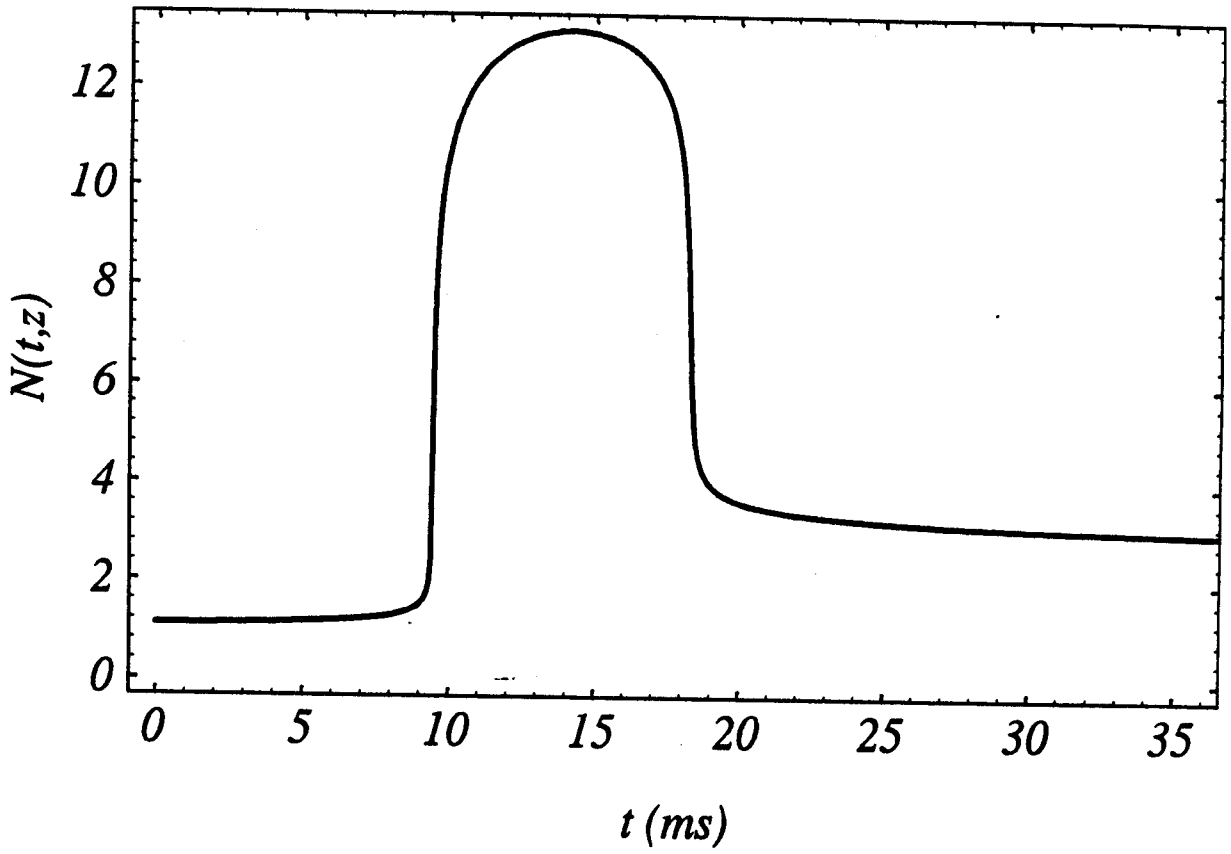

Fig. 3

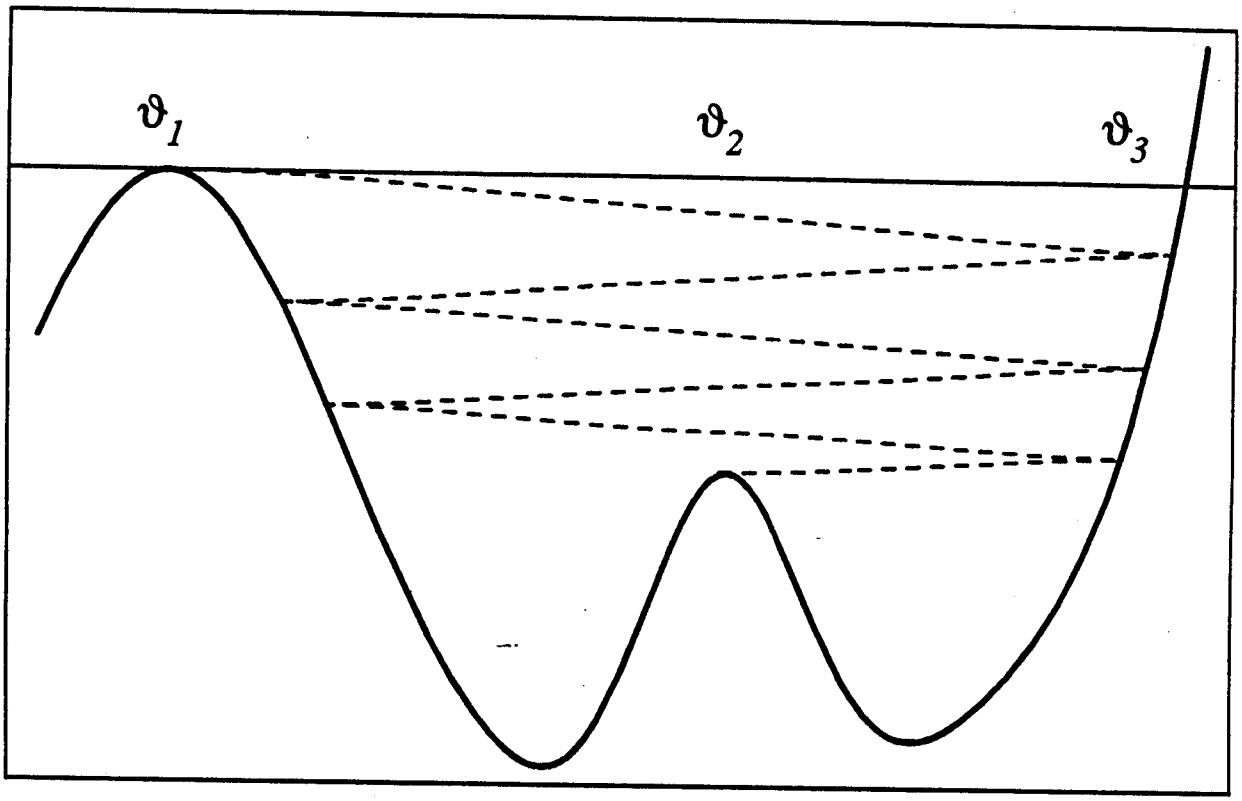

Fig. 4